J. Astrophys. Astr. (1994) **15,** 329–341

Pulsar Observations at Decametric Wavelengths using a Swept-frequency Dedisperser

A. A. Deshpande & V. Radhakrishnan *Raman Research Institute, Bangalore 560 080, India*

Received 1994 July 28; accepted 1994 August 30

Abstract. In this paper, we describe pulsar observations at decametric wavelengths using the Gauribidanur Radio Telescope made subsequent to our earlier measurements (Deshpande & Radhakrishnan 1992). To improve the time-resolution in our measurements of pulse profiles, we have used the 'swept-frequency dedispersion' method with some modifications to suit its application at such low radio frequencies. We also present a new scheme that simplifies the calibration of the receiver gain characteristics. We present average profiles on four pulsars from these improved measurements at 34.5 MHz.

Key words: Pulsars—average profiles—dispersion.

1. Introduction

The observations of pulsar signals are increasingly affected at lower radio frequencies by a variety of propagation effects occurring in the intervening medium. This limits pulsar studies at low radio frequencies to only nearby, i.e. low dispersion measure, pulsars. At these frequencies, observations of pulsars with high dispersion measures are in principle possible if the scatter broadening is not too severe. Using a single-spectral-channel receiver, we were able to detect 8 pulsars at 34.5 MHz (Deshpande 1987; Deshpande & Radhakrishnan 1992, hereafter referred to as DR92). However, the apparent profile widths were dominated by the dispersion effects over the 30 kHz bandwidth used. Hence, it was clear that to obtain high time-resolution profiles with sufficiently wide bandwidths, one needs some suitable dedispersion method. In this paper, we describe our pulsar observations at 34.5 MHz made using swept-frequency dedispersion (Deshpande 1987) with the Decameterwave Radio Telescope at Gauribidanur (GEETEE)*, India (Deshpande, Shevgaonkar & Sastry 1989). In the first part of this paper, the dedispersion method and the relevant observing setup is described. A new scheme for gain calibration, the procedures used for observation, data processing, and detection are also discussed. Average pulse profiles of four pulsars obtained from these observations are presented.

* This telescope is jointly operated by the Indian Institute of Astrophysics, Bangalore and the Raman Research Institute, Bangalore.

2. Swept-frequency dedispersion method

The pre-detection dedispersion method used by us involves a basic swept-frequency dedispersion procedure similar to that of Sutton *et al.* (1970) and McCulloch, Taylor & Weisberg (1979). In this method, the periodicity and the dispersed nature of the pulsar signals are used to our advantage. It can be shown, that due to the dispersion the pulsar signal at any instant in time gets mapped into the frequency domain. Therefore, a pulse profile over one full period could be obtained, if the intensity as a function of frequency can be measured over a finite bandwidth (Δf) given by,

$$\Delta f \sim kPf_0^3/\mathrm{DM} \tag{1}$$

where k = a constant, f_0 = center frequency of observation ($\gg \Delta f$), DM = Dispersion Measure, and P = Period of the pulsar.

However, such a spectral pattern sweeps across the frequency band at an approximate rate of ($-\Delta f/P$). In this scheme of dedispersion, the pattern is made to appear stationary in the frequency domain by also 'sweeping' the centre frequency of the receiver appropriately. The dispersed pulsar signal then results in a train of 'fixed' spectral features separated by Δf corresponding to the dedispersed pulse profiles. This requires that the centre frequency of observation be swept at a rate given by the dispersion relation, in practice the sweep being reset at intervals that are integral multiples of the pulsar period. Intensity patterns can be then measured with high spectral resolution using a suitable spectral line receiver. The maximum time-resolution obtained in this manner corresponds to the dispersion smearing over one spectral bin. This forms the basis of the method employed by us to dedisperse the pulsar signals and to enable observations with high time-resolution.

2.1 *The receiver setup*

Figure 1 shows a schematic for the receiver setup used for the present observations. There are two important components in such a setup, namely a sweeping local oscillator system and a high-resolution spectrometer. A suitable sweeping local oscillator system (SLOS) was specially built for this purpose. A detailed description of this system is given in Deshpande (1992), and we will briefly mention here only the main characteristic of the system relevant for this discussion.

This SLOS is given the dispersion measure and the period of a pulsar along with the choice of start frequency for the sweep. The maximum sweep bandwidth available is 1 MHz and is centred around 34·5 MHz. At these observing frequencies this SLOS is suitable for observations of pulsars with P/DM ratio smaller than 0.2 where P is in seconds and DM is in units of pc cm^{-3}. We have considered most of the pulsars detected at 102 MHz (Izvekova *et al.* 1979), as possible candidates for detection at 34.5 MHz, and find that the value of 1 MHz for the maximum sweep bandwidth is sufficient for most of them. The pulsars which need higher sweep bandwidths have either very low DMs or longer periods. Therefore, the effects of dispersion smearing are not very serious in their cases. The SLOS produces a staircase sweep matching closely with that described by the dispersion relation within an r.m.s. of about 250 Hz. The r.m.s. error in the sweep frequency produced should be less than the spectral resolution of the spectrometer used. The r.m.s. error in the present case results in an

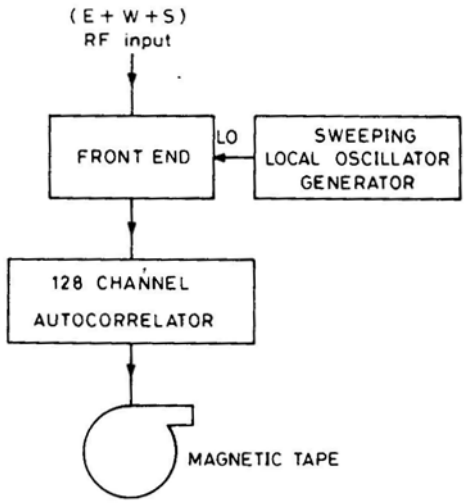

Figure 1. A simplified block diagram of the receiver setup.

additional smearing of about 8 milliseconds for DM= 100cm^{-3}pc. The staircase sweep has about 4000 steps of height 250 Hz on the average.

An existing 128 channel (complex) autocorrelation receiver provided high resolution intensity measurements in the frequency domain. (A detailed description of this receiver is given in Udayashankar & Ravishankar 1990). With a suitable choice of the baseband filter and appropriate sampling clock rate, the observing bandwidth (B) can be selected to give a spectral resolution of (B/256). A maximum sampling rate of 2MHz is possible with this receiver.

3. A new scheme for gain calibration

As discussed earlier, the intensity pattern in the spectral domain due to the pulsar signal can be made to appear stationary by the use of a suitable sweeping local oscillator system. Let us assume, that the SLOS frequency $f_{\text{out}}(t)$ is swept from f_s to f_e (such that $f_s > f_e$) in each interval equal to P starting from time $t = 0$ up to time $t = t_{\text{on}}$. The average intensity pattern at the output can be expressed in general as

$$\bar{I}(n) = \frac{1}{t_{\text{on}}} \int_0^{t_{\text{on}}} \left[\frac{1}{\delta f} \int_{-\delta f/2}^{+\delta f/2} |G_a(f_{\text{RF}})|^2 |G_b(f_{\text{LF}})|^2 [I_P(f_{\text{RF}}, t) + I_B(f_{\text{RF}}, t)] \, df \right] dt \qquad (2)$$

where n = bin index of the output intensity pattern, δf = resolution of the spectrum/ bin width, G_a = gain function of the telescope system upto the mixer stage, G_b = gain of the baseband filter, $I_P(f_{\text{RF}},t)$ = spectral power density of the pulsar signal at the input of the antenna, I_B (f_{RF}, t) = spectral power density of the background radiation, $f_{\text{RF}} = f_{\text{out}}(t) + n.\delta f + f, f_{\text{LF}} = n.\delta f + f,$ and $\delta f \ll (f_s - f_e) \ll f_{\text{out}}$.

If the interval (P') of each sweep is equal to the apparent period (P) of the pulsar and if the duration of observation, t_{on}, is an integral multiple of P, then the above

equation can be simplified to

$$\bar{I}(n) \simeq g(n)[\bar{I}_P(\phi_s(n)) + \bar{I}_B] \tag{3}$$

where

$$g(n) = \frac{1}{P}\int_0^P \left[\frac{1}{\delta f}\int_{-\delta f/2}^{+\delta f/2} |G_a(f_{\mathrm{RF}})|^2 |G_b(f_{\mathrm{LF}})|^2 \mathrm{d}f\right]\mathrm{d}t \tag{4}$$

and $\phi_s(n)$= longitude of the pulsar signal at the frequency (f_s + $n\delta f$) and at time t =0 $\bar{I}_p$ (ϕ_s (n))= time average of the intensity of the pulsar signal atlongitude $\phi_s(n)$,$\bar{I}_B$, = time average of the intensity of the background radiation.

We have assumed that over a small bandwidth δf all the above functions can be considered to be constant. It should be noted, that for obtaining the intensity profile corresponding to at least one period of the pulsar signal a total bandwidth of at least Δf (as in equation (1)) should be used. Further, to estimate the quantity [$\bar{I}_p$,($\phi_s(n)$), + $\bar{I}_n$], we need to know $g(n)$ to a sufficient accuracy. As the quantity $g(n)$ includes the antenna and the array component responses, it can be best measured by making observations *off* the source. In such a case, the measured intensities $\bar{I}_{\mathrm{off}}(n)$ are given by

$$\bar{I}_{\mathrm{off}}(n) \simeq \mathrm{g}(n)\,\bar{I}'_B \tag{5}$$

where $\bar{I}'_B$ = the background noise intensity *off* the source.

Thus the measured intensities can be treated as a scaled version of the function g(n). However, the accuracy to which $g(n)$ can be measured, i.e. $\Delta g(n)$, is given by

$$\Delta g(n) = \frac{\Delta I_{\mathrm{off}}(n)}{\bar{I}_{\mathrm{off}}(n)}\, g(n) \tag{6}$$

where

$$\Delta I_{\mathrm{off}}(n) = \frac{m\bar{I}_{\mathrm{off}}(n)}{\sqrt{\delta f\, t_{\mathrm{off}}}} \tag{7}$$

m= a receiver dependent constant and t_{off} = the duration of such an observation.

Noting that in practice $I_p \ll I_B$, the uncertainty in the estimation of $\bar{I}_p$,($\phi_s(n)$) can be shown to be

$$\Delta I_P \propto \frac{\bar{I}_B}{\sqrt{\delta f}}\left[\frac{1}{t_{\mathrm{on}}} + \frac{1}{t_{\mathrm{off}}}\right]^{1/2} \tag{8}$$

where $\bar{I}_B$ is assumed to be equal to $\bar{I}'_B$ for simplicity.

If the *off-source* measurements are made by switching the beam *on* and *off* the source at a fast rate, then t_{on} = t_{off} typically. The switching reduces the effective observing time on the source by a factor of 2. This will worsen the attainable sensitivity by a factor of 2, even if we ignore other problems associated with the fast beam switching. Another way is to make such *off-source* observations over a separate time span. Then the uncertainties in determining $g(n)$ *can* be considered negligible if $t_{\mathrm{off}} \gg t_{\mathrm{on}}$. Thus the *off-source* measurements need to be made over typically 3–4 hours. Apart from such large overheads in the observing time, it is also required that $g(n)$ does not change over the entire interval of observation. It should be noted that the function $g(n)$ will be different for different values of the period and the dispersion measure. These factors make such *off-source* measurements extremely time consuming.

Here, we suggest a different scheme for gain calibration, wherein we avoid the need for an accurate estimation of $g(n)$.

We have noted already that the spectral intensity pattern due to the pulsar signal is made to appear stationary if the appropriate LO sweep is reset only at invervals of the integral number (L) of the apparent period (P) of the pulsar. In our case,we will concentrate on the case when L= 1. Any deviation ΔP in such reset intervals causes the spectral intensity pattern to drift at a rate given by

$$\left(\frac{\mathrm{d}f_r}{\mathrm{d}t}\right)_d = \left(\frac{\Delta P}{P}\right)\cdot\left(\frac{\mathrm{d}f}{\mathrm{d}t}\right)_{sw} \tag{9}$$

(where $(\mathrm{d}f/\mathrm{d}t)_{sw}$ = the sweep rate of the SLOS and $\Delta P \ll P$.

If the intensity pattern is averaged for a long time without accounting for such a drift, the pulsar features would be smeared over the total drift. However, if the intensity patterns are sampled frequently enough and are averaged suitably by accounting for the drift, the average output intensity would have an equivalent gain $g'(n)$, given by

$$g'(n) = \frac{1}{t_{on}}\int_0^{t_{on}} g(n'(t))\,\mathrm{d}t \tag{10}$$

where

$$n'(t) = \mathrm{INT}\left[\mathrm{Frac}\left[\frac{(n+n_d(t))}{(\Delta f/\delta f)}\right]\cdot\left(\frac{\Delta f}{\delta f}\right)\right] \tag{11}$$

$n_d(t)$ is the number of bins by which the pattern drifts in time t and is given by

$$n_d(t) = \left(\frac{\mathrm{d}f}{\mathrm{d}t}\right)_d\cdot\left(\frac{t}{\delta f}\right) \tag{12}$$

It can be shown, that if

$$n_d(t_{on}) = N_d\left(\frac{\Delta f}{\delta f}\right) \tag{13}$$

where N_d = integer number of drift cycles (i.e. = 1,2,...) then the effective gain $g'(n)$ will have a constant value, say $\bar{g}$, irrespective of n. This condition implies that

$$t_{on} = \frac{N_d P^2}{\Delta P} \tag{14}$$

Thus, with suitable choices of t_{on}, ΔP and N_d, it is possible to obtain an average intensity pattern for the pulsar signal without needing an accurate measurement of $g(n)$. It should be pointed out at this stage, that if there exist large deviations within the gain function $g(n)$ from its means value, then the final signal-to-noise ratio attainable in the above scheme is reduced. In such a case, a crude estimate of $g(n)$ can be used to divide the individual intensity patterns before averaging, so as to reduce the deviations in the effective gain function drastically. The modified gain function is given by

$$g1(n) = \frac{g(n)}{g_0(n)} \tag{15}$$

where $g_0(n)$ = the crude estimate of $g(n)$.

The crude estimate $g_0(n)$ can be obtained by averaging the indivdual patterns without accounting for the del berate drift $(df/dt)_d$ and be used after suitable normalization Further, if should be noted, that the above solution is based on an assumption that to intensity pattern for the pulsar signal does not fluctuate during the observation However this a assumption does not strictly hold good in practice. Then, the final intensity pattern would correspond to the weighted (w.r.t. $g1(n)$) mean intensity pattern of the pulsar signal. The final profiles would be affected most due to this problem if N_d=1. Assuming that the fluctuations are random, this problem can be overcome to a great extent by choosing higher values of N_d. For given values of t_{on} and P,this would imply (from equation 14) higher values of ΔP. However any nonzero value of ΔP would cause additional smearing typically of the order of $\delta t = (\Delta P/P)\ T_s$; where T_s =the (read-out) sampling interval. This smearing should be as small as possible. If the sampling interval, T_s, is comparable to P, then this condition can be stated otherwise as $(\Delta P/P) \ll (\delta f/\Delta f)$. Therefore, the value of ΔP needs to be optimized with respect to N_d and δt

with a suitable choice of the above mentioned parameters, the output intensity pattern, $I(n)$, can be expressed as

$$\bar{I}(n) \simeq \bar{g}(\bar{I}_P(\phi_s(n)) + \bar{I}_B) \tag{16}$$

As $\bar{I}_p \ll \bar{I}_B$, a flux calibration could be obtained almost directly if an independent estimate of $\bar{I}_B$ is available. Apart from avoiding accurate measurements of the gain function g(n) on a routine basis, the above scheme has some more interesting and important advantages. In the conventional scheme, where $\Delta P = 0$, we need to observe over a bandwidth equal to or greater than Δf, to obtain the intensity pattern over one full period. It should be pointed out that the pulsar emission at low radio-frequencies may not be limited to the main pulse and the interpulse window alone (Bruck & Ustimenko 1976, 1977, 1979). This aspect makes it necessary to observe the intensity pattern corresponding to the full longitude range. The constraint in turn limits the resolution in time domain to P/N_{ch} in general, where N_{ch} is the number of spectral channels. However, our new calibration scheme readily provides a possibility of increasing the resolution beyond the above limit. In this scheme, if the observing bandwidth (B) is chosen smaller than Δf, then the time-resolution obtainable increases by factor $\gamma = \Delta f/B$. The observing band with can be decrease upto the limit when B/N_{ch}. becomes equal to the r.m.s. error in the SLOS ouput frequency However, such an improvement in resolution is at the cost of reduction in the sensitivity by a factor of $1/\sqrt{\gamma}$ The other advantage, which is quite important but implicit in this scheme, is that of not requiring absolute synchronization of the sweep with respect to the arrival time of the main pulse in the pulsar signal. Thus we note that the case when $\Delta P \neq 0$, has many important advantages compared to the conventional case when $\Delta P = 0$. We have used this new scheme for the observations described in this paper.

4. Observations and data acquisition

In this section, we describe the procedures adopted for the pulsar observations using the above discussed schemes. The basic receiver set-up is shown m Fig. 1. It should be noted, that the autocorrelation receiver (ACR) accepts only one input signal. The

antenna outputs are available from both the EW array and S array (of the Gauribidanur 'T' shaped array) separately. The possible single inputs to ACR are namely the (E+W),S or (E+W+S). The choice of (E+W+S)is obvious for the ACR input, due to the high effective aperture area corresponding to it. The beam pattern corresponding to this (E +W+S) mode is quite complex, and can be described as

$$R_{(E+W+S)} = R_{(E+W)} + R_{(S)} + 2 \cdot R_{((E+W)\times S)} \tag{17}$$

where $R_{('x')}$ = the beam pattern in, '*x*' mode.

The first two terms on the right hand side of the above equation correspond to two orthogonal fan beams, while the last term corresponds to a pencil beam due to the correlation. Thus the resultant beam has an equivalent resolution much poorer compared to that in the case of correlation. This aspect does not pose any serious problem in the case of pulsar observations, as the probability of encountering a 'confusing' pulsar, with its period and DM very close to that for the pulsar of interest, in the total field of view is very small. In this mode, the tracking facility (Deshpande, Shevgaonkar & Sastry 1989) can also be used to obtain longer observing time. The single input (E + W + S) is obtained by combining the (E + W) and S signals with equal phases. Amplitudes of the E + W and the S inputs are adjusted, such that all the basic array elements contribute equally at the combiner output. The SLOS is used with suitable settings. The relevant value of the Dispersion Measure (DM) is set accurate to ± 0.005 cm^{-3} pc. The sweep reset period is set different from the apparent pulsar period, such that $(\Delta P/P) \sim 2 \times 10^{-3}$ typically. The starting frequency for the sweep is chosen suitably to centre the sweep approximately at 34.5 MHz. Different observing bandwidths (B) can be employed by using appropriate base band filters and the sampling clock frequency. The choice of this bandwidth determines the signal-to-noise ratio and the time-resolution obtainable in the output profiles for given pulsar parameters. The online integration time (τ_{on}), to average the auto-correlations, can be selected in the range $(2^{12} \rightarrow 2^{19})/f_{clk}$ where f_{clk} is the sampling clock frequency. The averaged correlations available at the output of this receiver are recorded on a magnetic tape. The sampling time, T_s, is equal to the on-line integration time (τ_{on}). In order to recover the absolute amplitude information lost due to the one-bit processing in the receiver, it is required to measure the signal power at the input of the zero-cross detectors. Outputs of four threshold detectors/ integrators (Udayashankar & Ravishankar 1990) employed for this purpose are also recorded along with the autocorrelations.

5. Data processing and detection

The data recorded during these observations consist of the autocorrelation function measured using the autocorrelation receiver-SLOS combination. The autocorrelations available are *normalized one-bit autocorrelations* at positive delays. The processing involves the following steps.

5.1 *Estimation of the spectra*

The one-bit correlation values are translated to the corresponding analog correlations through the Van-vleck relation.

$$\rho_a = \mathrm{SIN}\left(\frac{\pi}{2}\rho_c\right) \tag{18}$$

where ρ_c is the normalized one-bit correlation and ρ_a is the corresponding normalized analog correlation. This computation is performed for both real and imaginary parts of the correlations separately As already noted, the absolute amplitude information is lost in one-bit processing. However, if estimates of the total Signal power at the input of the zero-cross detector are available, as in the present case it is possible to recover the absolute amplitude information. The available estimates of the total power are used to multiply the normalized correlations to obtain the amplitude calibrated (unnormalized) values of the autocorrelations. The amplitude calibrated (in-phase and quadrature) correlations obtained for positive delays are used to get a complex Hermitian symmetric autocorrelation function. The autocorrelation function and the power spectrum of the signal form a Fourier transform pair. We use a 256-point Fast Fourier Transform (FFT) routine to transform the autocorrelation function to a power spectrum. Thus, a power spectrum is obtained corresponding to each of the autocorrelation functions sampled at every interval of the on-line integration.

5.2 *Average band shape*

The power spectra obtained over the observing interval are averaged together to obtain a function representing the average gains of the spectral bins, i.e. the gain function $g_o(n)$ of the antenna-receiver combination. It should be noted that the band shape thus obtained is not expected to be affected by the presence of pulsar signals on the average, because of the deliberate slow drift of the spectral pattern due to the pulsar signal.

5.3 *Pulsar profiles*

Each of the power spectra contains a spectral pattern due to the observed pulsar signal. This pattern is weighted by the gain function of the receiver across the spectral band. We use the gain function $g_o(n)$ obtained earlier to divide each power spectrum so as to roughly equalize the receiver gain across the spectral pattern. The spectrum thus obtained ideally has a dc pedestal on which the pulsar pattern buried in the background noise is placed. The value of the dc pedestal corresponds to the average power due to the background noise (say, P_{noise}). Using an appropriate dispersion law, the spectral pattern is converted to a time domain pattern where the sampling becorncs, in general, non-uniform. This procedure is repeated for all power spectra obtained at regular intervals of the on-line integration. The final apparent time series obtained over the total observing interval (t_{on}) is then averaged synchronous to the apparent period of the pulsar. The bin-width in the time domain is chosen as close as possible to the dispersion smearing over one spectral bin, such that the apparent period is divktei into integral number of bins. Using similar procedure as described in DR92, an average profile over a two-period stretch is obtained and is tested for significant detction of two pulses which should be separated by exactly one period. The threshold for significant detection is chosen to be equal to three times the r.m.s.

deviations due to the noise in the two-period stretch. The value for the r.m.s. noise deviations (σ) is computed as

$$\sigma = \frac{mP_{\text{noise}}}{\sqrt{\bar{C}\tau_{\text{on}}\delta f}}, \tag{19}$$

where $\bar{C}$ is the mean number of samples averaged per bin. In case of a successful detection, the final average profile is obtained by combining the two halves of the corresponding two-period stretches. In an ideal case, the final profile has a flat baseline corresponding to the average noise power per bin (P_{noise}). However, in practice, the baselines are generally not flat. Such baselines can result from any low level broadcast interference within the observing band when swept across the band over Δf, and cannot be expected to have any systematic shape in general. For the purpose of baseline estimation the data in the off-pulse region of the profile was used and a lower order polynomial was fitted. The smooth baseline then was subtracted from the raw profile.

6. Results and discussion

Using the observational and the data processing procedures described in this paper, observations were attempted in the directions of more than 20 pulsars. The dispersion measures for these pulsars are in the range 12.4to 79 cm^{-3} pc. An observing band width (B) of 333 KHz and a sampling interval (read-out interval, T_s) of 1.57 second were used in all cases. In the cases of only four pulsars, namely PSRs 0628 — 28,0834 + 06, 0943 + 10 and 1919 + 21, was it possible to satisfy the detection criterion. For these pulsars, average pulse profiles were obtained with good signal-to-noise ratio.

As the values of Δf for three out of the four pulsars are larger than 333 KHz, it was possible to improve the time-resolution beyond (P/256) in these cases. The results obtained demonstrate the usefulness of the method employed to detect highly dispersed pulsar signals with high time-resolution.

The profiles obtained from these observations are shown in Fig. 2. The profiles presented are smoothened additionally over 3 bins for PSR 1919 + 21 and over 10 bins in other cases. The, error bars correspond to five times the standard deviations due to noise.

6.1 *PSR 0628 28* (*Fig. 2a*)

This pulsar with a dispersion measure of 34.56 cm^{-3} pc was detected at such a low frequency in our earlier observations (DR92). Note the weak emission feature at about 185° longitude, which can be easily distinguished from the rest of the off-pulse baseline (Fig. 2a). If this feature is due to interpulse emission, then the ratio of the energy of the interpulse to that of the main pulse is about 0.15. However, more observations made to confirm the possible interpulse emission did not show this feature. Therefore, at best, it suggests sporadic interpulse emission. The observed width at half-maximum of the main pulse is about 125 milliseconds.

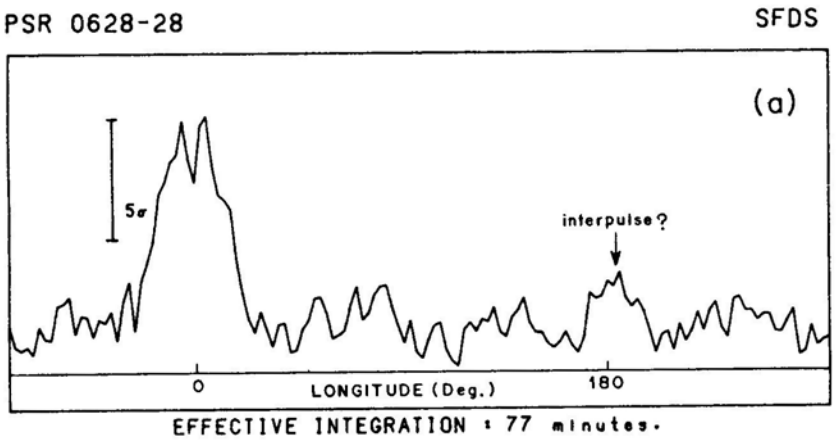
PSR 0628-28
SFDS
(a)
5σ
interpulse?
0
LONGITUDE (Deg.)
180
EFFECTIVE INTEGRATION : 77 minutes.

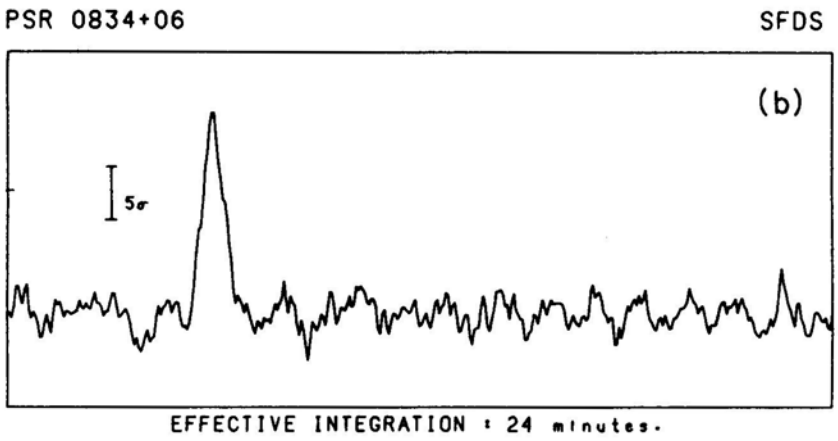
PSR 0834+06
SFDS
(b)
5σ
EFFECTIVE INTEGRATION : 24 minutes.

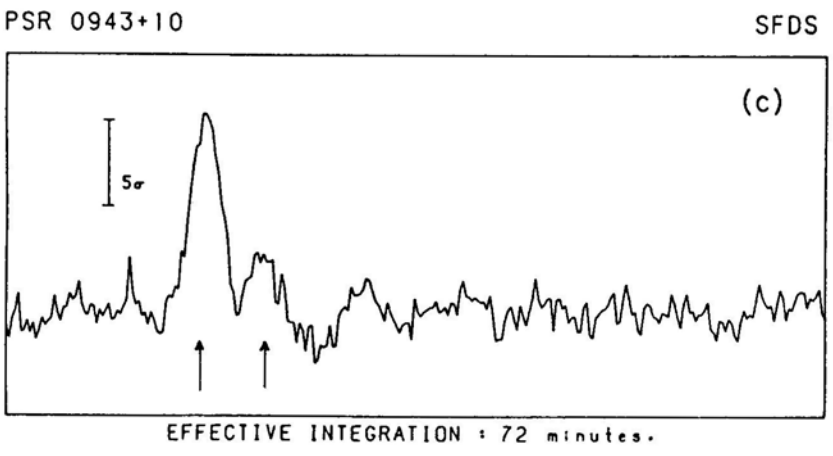
PSR 0943+10
SFDS
(c)
5σ
EFFECTIVE INTEGRATION : 72 minutes.

Figure2 (a,b,c).

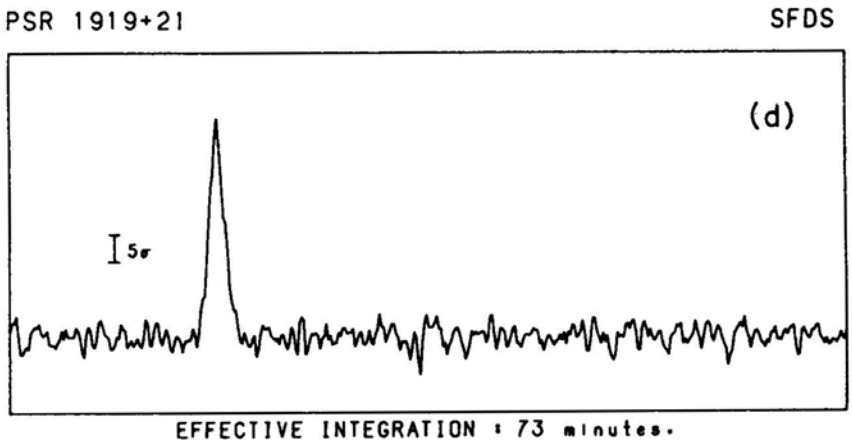

Figure2(d).

Figure 2. The average pulse profiles for (**a**)**:** PSR 0628 –28; (**b**)**:** PSR 0834 + 06; (**c**)**:** PSR 0943 + 10 and (**d**)**:** PSR 1919 + 21 observed at 34.5 MHz using the swept-frequency dedisperser.

6.2 *PSR 0834 + 06* (*Fig. 2b*)

A high time-resolution profile obtained in the present observations (on one day) is shown in Fig. 2b. The improvement in the time-resolution due to the SFDS in comparison with our earlier measurements (DR92) is quite striking. The observed width in this case is approximately 36 milliseconds. The average profile does not show any significant interpulse emission contrary to that reported at 25 MHz (Bruck & Ustimenko 1976, 1979), but is consistent with the observations by us earlier (Deshpande & Radhakrishnan 1990 and also DR92) and with those by Phillips & Wolszczan (1989).

6.3 PSR *0943 + 10* (*Fig. 2c*)

Figure 2c shows a high resolution profile obtained by combining the data on two days. Suleimanova & Izvekova (1984) have reported mode changing for this pulsar at 62 and 102 MHz. The pulse profile, obtained by us after averaging many days' data, seems to suggest that only one of the two modes (namely, B and Q) discussed by Suleimanova & Izvekova (1984) becomes prominent at decametric wavelengths. This (B) mode is observed to have two peaks with an intensity ratio of 3.5:1 at 102 MHz. This intensity ratio appears to be about the same at 34.5MHz.However, the separation of the two components has increased to about 80 milliseconds at the present frequency from 31 milliseconds at 102 MHz. This suggests to us that the separation is proportional to $(wavelength)^{0.9}$. It is worth pointing out that at about a meter wavelength this pulsar has a 'conal single' profile (Rankin 1993) suggesting that thesight-line cuts the emission cone tangentially. The fact that no measurements on this pulsar at frequencies above 610 MHz are reported suggests that the sight-line maybemissing the emission beam completely. The profile and the pulse-intensity evolution in the frequency range 0.6–1 GHz is therefore worth investigating. It is also

worth noting that the pulse energy spectrum for this pulsar is seen to be still rising even upto 34.5 MHz (DR92). This happens to be the first case where the spectrum for a long period pulsar does not have a turnover even down to 34.5 MHz. Investigation of the spectrum and pulse profile of this pulsar at frequencies below 34.5MHz would be of interest.

6.4 *PSR 1919 + 21* (*Fig. 2d*)

The pulse profile on this pulsar (Fig. 2d) has the best longitude resolution obtained by us so far. The observed pulse width is about 30 msec implying that the intrinsic pulse width is smaller than that at high frequencies. This is consistent with the spectral behaviour of the pulse width of this pulsar reported by Slee, Bobra & Alurkar (1987) where they find (from the data at and above 80 MHz) that the pulse width decreases at lower frequencies. Again, we do not find any significant interpulse emission in the profiles obtained by us on this pulsar whereas significant interpulse emission had been reported at and below 25 MHz (Brück & Ustimenko 1977, 1979).

7. Summary

In this paper, we have described the swept-frequency dedispersion method adapted for pulsar observations at low radio-frequencies. Using it we have been able to detect finer details in the pulse profiles than were possible earlier at such a low frequency. The dispersion smearing in the worst case (i.e. DM = 34.36 cm^{-3} pc) is only about 9 milliseconds. Such smearing can be further reduced by observing with bands narrower than that (333 KHz) used for the present observations. The subsequent loss in the signal-to-noise ratio, however, should be recovered by observing over longer time spans.

Lastly, regarding the interpulse emission, we notice no significant emission beyond the main pulse window in those cases where significant interpulse emission was claimed to have been detected at and below 25 MHz.

Acknowledgements

We wish to acknowledge the help and cooperation from T. S. Ravishankar, G. N. Rajasekhar and H. A. Ashwathappa during the observations. A. A. D. thanks R. Nityananda, Ch. V. Sastry and N. Udayashankar for many useful discussions.

References

Bruck, Yu. M., Ustimenko, B. Yu. 1976, *Nature,* **260,** 766
Bruck, Yu. M., Ustimenko, B. Yu. 1977, *Astrophys. Space Sci.,* **51**, 225
Bruck, Yu. M., Ustimenko, B. Yu. 1979, *Astr. Astrophys.,* **80**, 170.
Deshpande, A. A. 1987, *Ph. D. Thesis,* Indian Institute of Technology, Bombay.
Deshpande, A. A. 1992,J Astrophys.Astr., **13,** 167.

Deshpande, A. A., Radhakrishnan, V. 1990, '*The Magnetospheric Structure and Emission Mechanisms of Radio Pulsars, Proc. I AU Colloquium* **128**, (eds) T. H. Hankins, J. M. Rankin & J. A. Gil (Poland: Pedagogical University Press).
Deshpande, A. A., Radhakrishnan, V. 1992, *J. Astrophys. Astr.,* **13**, 151.
Deshpande, A. A., Shevgaonkar, R. K., Sastry, Ch. V. 1989, *Journal of I ETE,* **35**, 342.
Izvekova, V. A., Kuzmin, A. D., Malofeev, V. M., Shitov, Yu. P. 1979, *Soviet Astr.,* **23**, 179.
McCulloch, P. M., Taylor, J. H., Weisberg, J. M. 1979, *Astrophys. J.,* **227** L 133.
Phillips, J. A., Wolszczan, A. 1989, *Astrophys. J. Lett.* **344**, L69.
Rankin, J. M. 1993, *Astrophys. J.,* **405**, 285.
Slee, O. B., Bobra, A. D., Alurkar, S. K. 1987, *Austr. J. Phys.,* **40,** 557.
Suleimanova, S. A., Izvekova, V. A. 1984, *Soviet Astr.,* **28,** 32.
Sutton, J. M., Staelin, D. H., Price, R. M., Weiner, R. 1970, *Astrophys.* J., **159,** L89.
Udayashankar, N., Ravishankar, T. S. 1990, *J. Astrophys. Astr.,* **11**, 297.